

are not too different. Thus we believe that the inverted part is quite well established.

Accordingly the main error for $r(V)$ in Fig. 3 is due to the error in the $N(E)$ points where $\Delta E/E \sim 2\%$. This gives $\Delta r/r \sim 1\%$ from Eq. (1).

*Alexander von Humboldt postdoctoral Fellow. Present and permanent address: Istituto de Scienze Fisiche dell'Università, 16132 Genova, Italy.

¹M. Cavallini, L. Meneghetti, G. Scoles, and M. Yealland, *Phys. Rev. Lett.* **24**, 1469 (1970).

²P. E. Siska, J. M. Parson, T. P. Schäfer, and Y. T. Lee, *J. Chem. Phys.* **55**, 5762 (1971).

³J. M. Farrar and Y. T. Lee, *J. Chem. Phys.* **56**, 5801 (1972).

⁴R. K. B. Helbing, *J. Chem. Phys.* **50**, 493 (1969).

⁵H. D. Dohmann, *Z. Phys.* **220**, 229 (1969).

⁶M. G. Dondi, G. Scoles, F. Torello, and H. Pauly, *J. Chem. Phys.* **51**, 392 (1969).

⁷P. Cantini, M. G. Dondi, G. Scoles, and F. Torello, *J. Chem. Phys.* **56**, 1946 (1972).

⁸H. G. Bennewitz, H. Busse, H. D. Dohmann, D. E. Oates, and W. Schrader, *Z. Phys.* **253**, 435 (1972).

⁹O. Halpern and R. A. Buckingham, *Phys. Rev.* **98**, 1626 (1955).

¹⁰J. P. Aldridge and R. H. Davis, *Phys. Rev. Lett.* **19**, 1001 (1967).

¹¹W. H. Miller, *Chem. Phys. Lett.* **10**, 7 (1971).

¹²R. Helbing, W. Gaide, and H. Pauly, *Z. Phys.* **208**, 215 (1968).

¹³H. P. Butz, R. Feltgen, H. Pauly, H. Vehmeyer, and M. Yealland, *Z. Phys.* **247**, 60 (1971).

¹⁴D. Beck, H. Dummel, and U. Henkel, *Z. Phys.* **185**, 19 (1965).

¹⁵R. Feltgen, dissertation, Bonn, 1970 (unpublished).

¹⁶W. H. Miller, *J. Chem. Phys.* **51**, 3631 (1969).

¹⁷W. H. Miller, *J. Chem. Phys.* **54**, 4174 (1971).

¹⁸Calculations for the potentials m LJ-D (see Ref. 8) and ESMSV-II (see Ref. 3) give cross sections which are too small (deviations up to 10%) in the Ramsauer-Townsend region. To exclude systematic experimental errors, further scattering chamber measurements with improved experimental conditions at low energies are in progress.

¹⁹R. B. Bernstein and J. T. Muckermann, *Advan. Chem. Phys.* **12**, 389 (1967); for a more complete reference list see also Ref. 7.

²⁰D. E. Beck, *Mol. Phys.* **14**, 311 (1968).

²¹L. W. Bruch and I. J. McGee, *J. Chem. Phys.* **52**, 5884 (1970).

²²At low energies the derived potential fits slightly worse than the potential of Ref. 7 because the mean cross section is changed by the inverted potential part at higher energies where theory and experiment are forced to agree.

Electron Loss in High-Energy Oxygen-Ion Collisions*

D. Burch, H. Wieman, and W. B. Ingalls

Department of Physics, University of Washington, Seattle, Washington 98195

(Received 19 March 1973)

The 90° electron spectra from oxygen-ion single collisions with Ar have been measured at energies of 17 to 41 MeV and charge states of 3+ to 8+. A broad peak in the spectra is observed and identified as electrons lost from the incident ion. A simple model of the electron-loss process is described which supports the identification.

Fast heavy-ion-atom collisions result in the production of copious amounts of electrons. The energy spectra of the emitted electrons have been studied in detail for incident heavy-ion energies below 500 keV. Recent reviews of these measurements have been given by Ogurtsov¹ and by Rudd and Macek.² At observation angles of 90° or greater, the continuous electron spectra are found to be monotonic functions of the electron energy, decreasing nearly exponentially with increasing electron energy. Superimposed on the continuous backgrounds, monoenergetic electrons have also been observed from autoionization and Auger de-excitation of the target and projectile.

The subject of this Letter is the continuous

spectra in similar measurements at much higher energies—in particular, a prominent peak in these spectra which is unique to collisions at these energies. This peak is shown, on the basis of the incident energy and charge-state dependence, to be attributable to electrons knocked out of the incident ion. A simple model of the electron-loss process based on elastic electron scattering is described which semiquantitatively supports this identification.

We have measured the 90° electron spectra in single collisions of oxygen ions with several gases at energies of 17.5 to 40.8 MeV using charge states of 3+ to 8+. The oxygen beams were produced in the University of Washington's FN tan-

dem Van de Graaff accelerator. The intensities of the 30-MeV O^{3+} and O^{8+} beams were 100 nA; the intensities of the other beams used were 5 to 10 times higher. After energy and charge-state analysis, the beam traveled 10 m in a vacuum of $<2 \times 10^{-6}$ Torr and entered a differentially pumped gas-scattering cell. The target-gas pressure was $(4.6 \pm 0.2) \times 10^{-3}$ Torr measured with a Baratron capacitance manometer. The oxygen beam traversed 5 cm of gas at this pressure before reaching the center of the scattering region visible to the electron analyzer. Charge-exchange measurements³ have shown that less than 5% of the beam undergoes a charge-changing collision under these circumstances. Since the electron spectra which we report are dependent upon the incident-ion charge state, we were able to test the charge-state purity by measuring the target-pressure dependence on the electron spectra. The pressure-variation measurements were also used to determine the electron-energy dependence of the effective electron "absorption coefficients." The emitted electrons traveled 5 cm through the target gas to reach the analyzer vacuum chamber which was also differentially pumped to 2×10^{-6} Torr. The electrons were energy analyzed with a cylindrical-mirror electrostatic analyzer⁴ with a resolution of 1.4% full width at half-maximum. An SDS-930 computer was used to store the spectra and control the automated operation of the analyzer. The measurements were made at a laboratory angle of 90° with an acceptance angle of $\pm 5^\circ$.

Figure 1 shows the observed electron spectra in the energy range of 310 to 2100 eV from $O^{4+} + Ar$ at several O^{4+} energies. The spectra are shown normalized to the number of counts observed at 310 eV which was $\sim 10^4$ in each case. The shape and energy of the broad peak was found to be independent of target gas in collisions with O_2 , N_2 , Ne, and Ar. The spectra shown are raw data which have not been corrected for the transmission function of the analyzer ($1/E$), the scattering losses (absorption) in the target gas, or the Channeltron electron-detector efficiency. The nearly exponential component of these spectra is due primarily to the electrons the oxygen nucleus knocked out of the Ar atom. The broad peak, which appears at an energy slightly less than that corresponding to the incident-ion velocity, is attributed to the electrons that the Ar atom knocked out of the 2s shell of the incident O^{4+} ion. In the following we present the basis for this identification.

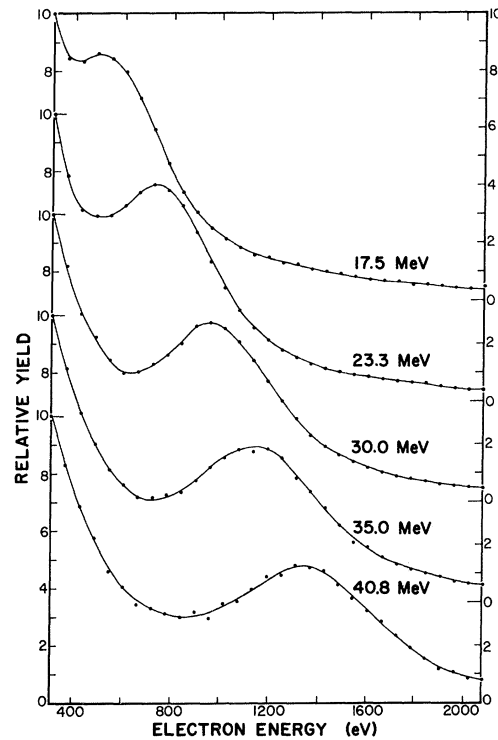


FIG. 1. Relative 90° electron yields in O^{4+} single collisions with Ar. The yields are shown normalized to the number of 310-eV electrons.

To lowest order the electrons on the incident ion may be considered to constitute merely a merged beam of electrons traveling with the velocity \vec{v}_i of the incident beam. The momentum distribution of the electrons which results from their binding to the ion is taken into account by adding to \vec{v}_i a component \vec{v} which is determined by the speed distribution $f_{ni}(v)$ characteristic of the outermost shell of the ion. An electron with velocity $\vec{v}'' = \vec{v}_i + \vec{v}$ is then considered to scatter elastically to the angle of observation θ' off the target atom which is represented by a screened Coulomb potential. The double-differential electron yield can then be determined, by integrating over the velocity distribution, as

$$dE' d\Omega' \frac{d^2\sigma}{dE' d\Omega'}(E', \theta')$$

$$= \int_{\Omega''} \frac{d\sigma}{d\Omega'}(\vec{v}'', \vec{v}') F(\vec{v}'') d\vec{v}'' d\Omega'', \quad (1)$$

where

$$F(\vec{v}'') d\vec{v}'' = \frac{f_{ni}(v)}{4\pi v^2} \frac{v''}{m} dE'' d\Omega'', \quad (2)$$

with $\frac{1}{2}mv''^2 = E'' = E'$ and

$$\frac{d\sigma}{d\Omega'}(\vec{v}'', \vec{v}') = \left(\frac{Ze^2}{E'}\right)^2 \frac{1}{(4 \sin^2\theta/2 + \theta_0^2)^2} \quad (3)$$

Equation (3) is the electron elastic-scattering cross section for a screened Coulomb potential⁵ $V(r) = (Ze^2/r) \exp(-r/R)$. θ is the angle between \vec{v}'' and \vec{v}' ($\cos\theta = \cos\theta' \cos\theta'' + \sin\theta' \sin\theta'' \cos\varphi''$), and θ_0 is the minimum scattering angle determined by the screening radius R and the de Broglie wavelength of the scattered electron⁵: $\theta_0 = \lambda/R$ and $R = a_0 Z^{-1/3}$. To analyze the O^{4+} data we have used the normalized speed distribution $f_{2s}(v)$ determined from the Fourier transform of

the 2s-hydrogenic wave function:

$$f_{2s}(v) = \frac{128}{\pi} \frac{v_0^5 v^2 (v^2 - v_0^2)^2}{(v^2 + v_0^2)^6}, \quad (4)$$

where $\frac{1}{2}mv_0^2 = 113.9$ eV, the binding energy⁶ of the last electron in O^{4+} .

Figure 2 shows the results of Eq. (1) evaluated numerically at $\theta' = 90^\circ$ compared with the relative experimental cross sections after the subtraction of a background determined from the low- and high-energy portions of the 40.8- and 17.5-MeV spectra, respectively. The present relative-yield measurements do not give information about the low-energy tail predicted by the model. For a given speed distribution the magnitude of this tail depends only on the screening radius R . The experimental data have been normalized to the peak heights in each case. It can be seen that this model does account for the shift below the incident velocity and also for the shape of the peak.

The shape of the peak does reflect the speed distribution of, specifically, the 2s shell. This is shown in the 30-MeV data of Fig. 2 where the broader 1s distribution has been used in place of Eq. (4) while keeping the binding energy fixed at 113.9 eV. It is interesting to speculate that measurements of this type might be developed to determine momentum distributions for specific electron shells. Data of this type are very rare and currently limited to results obtained in difficult coincidence measurements.⁷

Figure 3 shows the spectra from oxygen-ion collisions at a fixed energy and varying charge state. These results provide further evidence

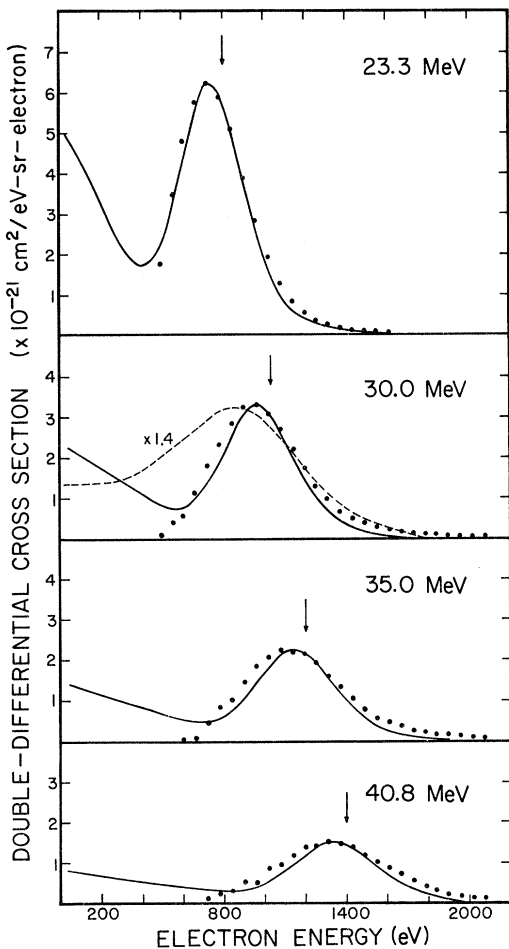


FIG. 2. Theoretical double-differential electron-loss cross sections at 90° compared to the experimental data normalized at the peak maximum in each spectrum. The arrow indicates the electron energy corresponding to the incident-ion velocity. The dashed curve in the 30-MeV spectrum results from a 1s speed distribution with a 2s² binding energy. The present experimental data do not give information about the low-energy electron yields.

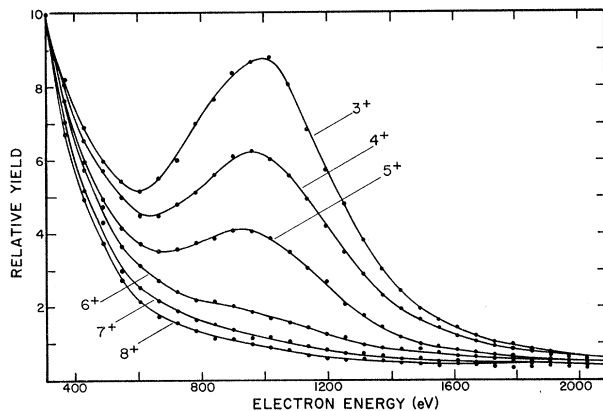


FIG. 3. Relative 90° electron yields in 30-MeV oxygen-ion single collisions with Ar for various charge states. The yields are shown normalized to the number of 310-eV electrons.

that the peak electrons originate from the L shell of the incident ion. The peak disappears when only K -shell electrons are left on the ion, and the intensity increases with increasing L -shell occupation. The small indication of the peak in the $6+$ data could be attributed to a small O^{5+} contamination of the beam.

Equation (1) can be integrated over all emitted electron energies and emission angles (E' , θ') to yield a total electron-loss cross section. This has been done for 30-MeV $O^{4+} + Ar$. The result is a factor of 8 higher than the measurements of Macdonald and Martin.³ We note, however, that Eq. (1) predicts a strongly forward peaked cross section. At forward angles the magnitude of the cross section is sensitive to the screening radius R . For example, a value of $R = 0.5a_0Z^{-1/3}$ results in good agreement with experiment ($5 \times 10^{-17} \text{ cm}^2$). This value of R is not unrealistic and, further, would not influence the 90° fits shown in Fig. 2.

Considerably more measurements, in particular absolute cross sections, are necessary to determine the utility of such a simple model of the electron-loss process. Most desirable would be coincidence experiments which measure the electron spectrum associated specifically with electron-loss events, e.g., in O^{4+} collisions, the spectrum in coincidence with the emerging O^{5+} ions. The electron intensity at energies below the peak could then be determined which would yield information about the effective screening and the high-velocity tail of the speed distribution. There is at present very little data available on electron production by high-energy heavy ions.⁸ Many laboratories are, however, preparing to make such measurements. The prominence of the electron-loss peak is unique to the fast heavy-ion collisions which can be studied at Van de Graaff facilities where wide ranges of heavy ions, energies, and charge states are available. Studies of the electron-loss process via electron spectroscopy should provide very sensitive tests of electron-loss theories.⁹

A primary motivation of electron measurements at high energies is the study of Auger spectra. In heavy-ion collisions the Auger groups are very broad in energy as a result of the multiple ionization created in the collision.⁸ Studies of the elec-

tron-loss spectra will be quite important in understanding the incident energy and charge-state dependent backgrounds to be expected.

We should add that the electron-loss peak has also been observed recently in other collisions: 0.6- to 1.5-MeV $H_2^+ + H_2$,¹⁰ 3-MeV $He^+ + Ne$,¹¹ and 140- and 150-keV $He + He$.¹² These last results show that the peak can be observed at lower energies in light-ion-atom collisions even though it is less pronounced because of high backgrounds.

It is a pleasure to thank Professor L. Wilets for many discussions which were very helpful in completing the analysis of this data. Stimulating discussions with Professor R. Vandenbosch are also gratefully acknowledged.

*Work supported in part by the U. S. Atomic Energy Commission.

¹G. N. Ogurtsov, *Rev. Mod. Phys.* **44**, 1 (1972).

²M. E. Rudd and J. H. Macek, in *Case Studies in Atomic Collisions*, edited by E. W. McDaniel and M. R. C. McDowell (North-Holland, Amsterdam, 1973).

³J. R. Macdonald and F. W. Martin, *Phys. Rev. A* **4**, 1965 (1971).

⁴J. S. Risley, *Rev. Sci. Instrum.* **43**, 95 (1972).

⁵See discussion and references in J. D. Jackson, *Classical Electrodynamics* (Wiley, New York, 1962), p. 451; C. J. Powell, in *Methods of Experimental Physics*, edited by L. Marton (Academic, New York, 1963), Vol. 7, Part B, p. 290; R. E. Burge and G. H. Smith, *Proc. Phys. Soc., London* **79**, 673 (1962).

⁶C. E. Moore, *Ionization Potentials and Ionization Limits Derived from the Analysis of Optical Spectra*, U. S. National Bureau of Standards, National Standard Reference Data Systems-34 (U. S. GPO, Washington, D. C., 1970).

⁷R. Camilloni, A. G. Guidoni, R. Tiribelli, and G. Stefani, *Phys. Rev. Lett.* **29**, 618 (1972); E. Weigold, S. T. Hood, and P. J. O. Teubner, *Phys. Rev. Lett.* **30**, 475 (1973).

⁸D. Burch, W. B. Ingalls, J. S. Risley, and R. Heffner, *Phys. Rev. Lett.* **29**, 1719 (1972).

⁹H. D. Betz, *Rev. Mod. Phys.* **44**, 465 (1972).

¹⁰W. E. Wilson and L. H. Toburen, *Phys. Rev. A* (to be published).

¹¹N. Stolterfoht, D. Schneider, and D. Burch, unpublished.

¹²F. D. Schowengerdt, S. R. Smart, and M. E. Rudd, *Phys. Rev. A* **7**, 560 (1973).